

PROPER MOTIONS AND VARIABILITY OF THE H₂ EMISSION IN THE HH 46/47 SYSTEM

Milena Micono^{1,2}, Christopher J. Davis^{1,3}, Thomas P. Ray¹, Jochen Eislöffel⁴ & Matthew D. Shetrone⁵

¹School of Cosmic Physics, Dublin Inst. for Adv. Studies, 5 Merrion Square, Dublin 2, Ireland

²Dipartimento di Fisica Generale dell'Università, Via Pietro Giuria 1, I-10125 Torino, Italy

³Joint Astronomy Centre, 660 N. A'ohōkū Place, University Park, Hilo, Hawaii 96720, U.S.A.

⁴Thüringer Landessternwarte Tautenburg, Sternwarte 5, D-07778 Tautenburg, Germany

⁵European Southern Observatory, Alonso de Cordova 3107, P.O. 19001, Santiago 19, Chile

ABSTRACT

We report here on the first proper motion measurements of molecular hydrogen emission features in the Herbig-Haro 46/47 outflow. Assuming a distance of 350 pc to this flow, the inferred tangential velocities range from a few tens to almost 500 km s⁻¹. The highest velocities are observed for H₂ knots either in, or close to, the jet/counterjet axes. Knots constituting the wings of the large scale H₂ bow (see, for example, Eislöffel et al. 1994) are found to move much more slowly. These results appear to be in agreement with recent numerical simulations of H₂ emission from pulsed jets. We also report the first detection of variability in H₂ features for a young stellar object (YSO) outflow. It was found that several H₂ knots significantly changed their luminosity over the 4 year timebase used to conduct our study. This is in line with current estimates for the cooling time of gas radiating shocked H₂ emission in YSO environments.

Subject headings: ISM: jets and outflows — stars: formation — stars: mass loss

1. Introduction

Although low mass star formation is accompanied by a diverse range of outflow phenomena evident at many wavelengths, it seems likely that the primary driving flow in each case is a Herbig-Haro (HH) jet (see, e.g., Padman, Bence & Richer 1997). Such jets were first discovered by Mundt & Fried (1983) and for a general review of their properties the reader is referred to Edwards, Ray & Mundt (1993). In regions of low extinction, HH jets can be observed optically in a number of emission lines, e.g. the [SII] $\lambda\lambda 6716, 6731$ doublet. In those cases where the jets are more deeply embedded, however, near-infrared H_2 emission is a much more useful tracer of HH flows (Eisloffel 1997) as evidenced, for example, by the dramatic H_2 $v=1-0$ S(1) $2.12\mu\text{m}$ images of Cep E (Eisloffel et al. 1996) and HH 212 (Zinnecker et al. 1997).

The general consensus is that the H_2 emission seen in young stellar object (YSO) outflows is due to radiative shocks. There has been, however, considerable debate in the literature over the nature of the shocks themselves with various observers preferring jump (J-)type and others magnetic continuous (C-)type shocks to explain their data (Eisloffel 1997). In particular J-shocks seem to be supported by excitation analysis (Gredel 1996; Everett 1997) whereas C-shocks are needed to model the observed wide ($50-100 \text{ km s}^{-1}$, FWHM) line profiles (e.g., Davis & Smith 1996). At the same time, an alternative scenario has been proposed by Taylor & Raga (1995) in which the H_2 emission is due to collisional excitement in turbulent boundary layers between the jet and its ambient medium. In such layers one expects to find flow velocities ranging from that of the ambient medium up to the velocity of the jet itself (Taylor & Raga 1995; Noriega-Crespo et al. 1997). Obviously in order to help distinguish between these different models, full kinematic data is required for the emitting regions. The combination of high resolution spectroscopic observations coupled with imaging at a number of epochs to determine proper motions and cooling timescales provides powerful constraints that can aid in selecting the correct model. With this in mind we have monitored, for a number of years, several well-known YSO outflows that are visible in the $2.12\mu\text{m}$ H_2 line. In order to obtain proper motion data, one requires IR camera images that contain sufficient reference stars. Such images have only been attainable in the past few years, so only now is it possible to make the first proper motion and, coincidentally, variability measurements of H_2 features.

The outflow we report on here, the HH 46/47 system (Dopita, Schwartz & Evans 1982) has as its source the low luminosity $L_* \approx 10L_\odot$ young stellar object (YSO) IRAS 08242-5050. This outflow is at the edge of a Bok globule, and powers not only a set of well-known optically-visible HH objects (e.g., Eisloffel & Mundt 1994) but also a bipolar molecular outflow (Olberg, Reipurth & Booth 1992). The northeastern (blueshifted)

portion of the flow is best observed optically (see, for example, the dramatic HST images in Heathcote et al. 1996). To study, however, the embedded “counterflow” as it ploughs into the Bok globule, one has to use infrared imaging. Such imaging, in the $2.12\mu\text{m}$ H_2 line, not only shows quite strikingly the “counterjet” but also an extensive bow shock that is clearly driven by the counterjet (Eisloffel et al. 1994).

The earliest detections of proper motions in HH 46/47 were made by Schwartz, Jones & Sirk (1984). More recently a comprehensive optical proper motion study of this region was carried out by Eisloffel & Mundt (1994). Here we report the first such study in H_2 emission, and one of the first measurements of proper motion of H_2 features in any YSO flow (see also Noriega-Crespo et al. 1997). Variability in H_2 emission is also detected here for the first time.

2. Observations and data reduction

Data obtained at 3 epochs (April 1993, November 1995 and April 1997), spanning a period of 4.0 yrs, were used to calculate proper motions in HH 46/47. These data have all been obtained at the ESO/MPI 2.2 m Telescope, using the IRAC2 near-IR camera which is equipped with a 256×256 pixel NICMOS 3 array and optics that yield a $0''.52/\text{pixel}$ scale. On each occasion, an H_2 $v=1-0$ filter ($\lambda = 2.121\mu\text{m}$, $\Delta\lambda = 0.04\mu\text{m}$) was employed. The same standard data reduction (sky-subtraction and dome flat-fielding) was carried out on each data-set; the observing sequence and data reduction are described in Eisloffel et al. (1994).

The reduced images were registered by the application of linear geometric transformations (translation, rotation and re-scaling) derived by comparing the positions of a number of field stars at different epochs. The positions of the stars were matched with an accuracy of the order of a tenth of a pixel. To measure the positions of the structures two methods were employed. For small and well defined knots, such as the jet/counterjet knots and similar bright substructures in more extended faint regions, we compared their positions at different times calculated using the intensity weighted first moments of the pixel values; the errors arising from this procedure were generally smaller than the error due to frame alignment. For more diffuse features, we calculated the shifts using a cross correlation technique, similar to that employed by Reipurth & Heathcote (1991), between boxes drawn around each structure at the different epochs. The errors associated with this procedure were estimated as typically 0.1 pixels ($\sim 0''.05$) for the brighter structures and 0.2 pixels ($\sim 0''.1$) for the fainter ones.

3. Results

The proper motions of the HH 46/47 H₂ knots, calculated using a linear least squares fit to the data points, are given in Table 1. They are also illustrated in Figs. 1 and 2, where we display, in contour form, an H₂ (+continuum) narrow-band mosaic of the HH 46/47 field from the April 1997 run plus separate finer scale images of the H₂ counterjet. We adopt a value of 350 pc for the distance to HH 46/47 in agreement with Eislöffel & Mundt (1994) and in line with more recent estimates of the distance to the nearby Gum Nebula (Franco 1990). In the direction of the counterflow, large tangential proper motions, in excess of 200 km s⁻¹, are measured for the knot at the apex of the bow (labeled a in Fig. 1 and lying in the vicinity of the optical knot HH 47C), the two knots within the bow, g and h, and the bright counter-jet knot, c-jet-d (see Fig. 2). Much lower proper motions (< 100 km s⁻¹) are measured along the bow wings (knots b – f). The H₂ proper motion measurements imply flow speeds along the counter-jet in the range 170–280 km s⁻¹, assuming its inclination angle with respect to the plane of the sky is $\sim 35^\circ$ as suggested by the optical data (Eislöffel & Mundt 1994). A comparison of the tangential velocities of the H₂ and optical knots in the counterflow shows that while both sets of features are moving in almost the same direction there is a tendency for the H₂ knots to be moving somewhat faster. For example knot a has a tangential velocity of 260 km s⁻¹ whereas the corresponding average velocity for the optical knots constituting HH 47C is approximately 150 km s⁻¹ (Eislöffel & Mundt 1994).

Turning to the northeastern section of the flow, this is far more prominent in optical forbidden line emission, e.g. [SII] $\lambda\lambda$ 6716,6731, than in H₂ emission. Close to the optical jet, however, that links the source and HH 46 with the HH 47A bow shock, there is a faint H₂ emission filament (x in Fig. 1) as well as an “arc” of H₂ emission towards HH 47A itself. Davis, Eislöffel & Smith (1996) associate the “arc” with the wings of the HH 47A bow shock (based on a comparison of its morphology with synthetic H₂ images of C-type bow shocks). The brightest peak in this H₂ arc, knot z, has a tangential velocity (67°, 184 km s⁻¹) that is very similar to its optical counterpart HH 47A0 (45°, 182 km s⁻¹) as measured by Eislöffel & Mundt (1994). The fainter H₂ filament, x, has a somewhat lower velocity, and interestingly seems to be moving almost northward, perhaps because of the lateral expansion of the outflow lobe itself (Fig. 1). Although there does not appear to be any corresponding optical feature in the same region, nevertheless there are a number of optical knots (A6 and A7) to the south of HH 47A which may also be expanding laterally (Eislöffel & Mundt 1994).

When comparing our H₂ images for the 3 epochs, it was noted that a small number of knots either appeared for the first time or faded from view within the 4 year period. Such knots were not used for proper motion measurements. An example can be seen in Fig. 2 where one of the knots in the counterjet, c-jet e, was seen both in the 1993 and 1995

images but disappeared by 1997. The fading and brightening of knots can, we believe, also cause anomalous proper motion results. For example the measured proper motion for knot c-jet b is not in the same direction as the counterjet and out of line with the motion of knots c-jet a and d. A cursory examination of Fig. 2, however, shows that in Nov. '95 knot c-jet b probably consisted of two marginally resolved sub-condensations, and that the most southwesterly one faded by Apr. '97. The net effect is, of course, to rotate the apparent proper motion vector more towards the source, as observed.

4. Analysis and Discussion

It is well known that molecular hydrogen dissociates in planar J and C-type shocks at velocities typically greater than ~ 25 and ~ 50 km s^{-1} respectively (Smith 1994). Given the large outflow speeds inferred by our proper motion measurements, and assuming the emission is from shocks, it is clear that the shocks are either oblique, e.g. as in the wings of a bow shock, and/or that they are caused by marginally faster material moving into somewhat slower gas. If the latter case applies, the shock speed can be quite low even though the velocity of the post-shock gas may be high. Numerical simulations of the expected H_2 emission from YSO outflows are only now becoming available (Smith 1991; Suttner et al. 1997) and in particular a simulation appropriate to the conditions for the HH 46/47 counterflow has recently been made (Downes & Ray 1998). Broadly speaking these simulations are in line with our observations. For example they predict low tangential velocities for the H_2 knots in the bow shock wings as is observed. The bow emission derives from entrained shocked ambient material and so, providing the pre-shock material is virtually stationary, we would not expect its post-shock velocity to be very high. On the other hand the H_2 emission within the flow itself can have much higher tangential velocities if it arises from marginally higher velocity material catching up with previously ejected gas. In this way, and providing there is sufficient H_2 present, the H_2 knots can reach tangential velocities close to that of the jet itself, i.e. several hundred km s^{-1} . The high tangential velocity of the H_2 emission close to apex of the bow (knot a) may arise in a slightly different way as it could come from the Mach disk (the shock “facing” the outflow source that decelerates the jet gas). Overlaying our H_2 plots onto the $[\text{SII}]\lambda\lambda 6716, 6731$ images of Eislöffel & Mundt (1994) shows that the H_2 emission is located just *behind* the $[\text{SII}]\lambda\lambda 6716, 6731$ bow as is consistent with this hypothesis. Moreover, if the jet is moving into lower density material near HH 47C, the Mach disk could be a low velocity shock. Under these conditions we might expect the excitation, rather than the dissociation, of molecular hydrogen. In this regard, it is interesting to note that for the corresponding feature in the northeastern flow, i.e. the Mach disk associated with HH 47A, Heathcote et

al. (1996) estimate its shock velocity to be about 35 km s^{-1} . Although this is close to the limit for the dissociation of H_2 , if we are dealing with a J-type shock, the conditions near HH 47C might be somewhat more favorable for the molecule’s survival.

In all of the observed knots and filaments, the cooling time for the heated H_2 molecules is expected to be short (≤ 2 years, assuming $n_{\text{H}_2} \geq 10^6 \text{ cm}^{-3}$ and $T_k \sim 2000 \text{ K}$; see for example Davis & Smith 1995). We therefore expect and, as we have already mentioned, indeed find that a number of H_2 knots appear and disappear on such timescales, and that the morphologies of some other knots change. One should also realize that, because the 4 year time span of our observations likely exceeds the cooling time, then our proper-motion measurements record the tangential motions of the shocks themselves rather than of the post-shock gas, since the shock-heated gas observed in our epoch-1993 observations will, by 1997, have radiatively cooled and will therefore no-longer be observable. Moreover, if in this time a shock front encounters lower-density, or perhaps even purely atomic gas, then emission observed in a particular region in 1993 could seemingly “disappear” by 1997. Indeed, the speeds, directions and apparent morphologies of the shocks themselves, as well as their ability to generate molecular line emission, are strongly depending on the conditions in the pre-shock gas, which may be inhomogeneous on small (even sub-arcsecond) scales.

5. Conclusions

Near-IR images, obtained over a 4 year period with the IRAC2 common-user instrument at ESO, Chile, were used to compute the proper motions of numerous H_2 knots and filaments in the HH 46/47 bipolar outflow. Tangential velocities ranging from $100\text{--}500 \text{ km s}^{-1}$ were recorded for the HH 47A bow shock and for knots in, or close to, the IR counter-jet. Lower velocities were measured along the bow shock wings in the counter-flow, in support of earlier interpretations of the overall flow morphology and recent numerical simulations of molecular jets. The measured tangential velocities of the H_2 features appear comparable in magnitude, and generally follow the trend of the corresponding optical features in the same regions. Variability is also observed in some knots, which change apparent “shape” or vanish altogether. This is a result of the fact that the cooling times associated with the observed molecular shock features are comparable to or shorter than the 4 year time-span of our observations.

ACKNOWLEDGEMENTS

We would like to thank the 2.2m team at ESO for their continued support with the use of IRAC2. M.M. wishes to acknowledge the warm hospitality and financial support from

DIAS where this work was carried out. Finally we would also like to thank the referee, Alex Raga, for his helpful comments.

TABLE 1
PROPER MOTIONS OF THE H₂ KNOTS IN HH 46/47

H ₂ Knot	Shift (arcsec/yr)	PA (degrees)	V_{tan}^1 (km s ⁻¹)
a	0.157(±0.011)	254.9(±3.8)	260
b	0.049(±0.011)	252.8(±12.3)	81
c ²	0.036(±0.011)	256.0(±16.5)	60
d	0.047(±0.004)	311.8(±5.1)	78
e	0.029(±0.004)	217.1(±8.2)	48
d+e ²	0.031(±0.011)	285.5(±19.6)	51
f	0.024(±0.012)	201.9(±26.1)	40
g	0.250(±0.021)	266.7(±4.8)	414
h	0.296(±0.021)	254.0(±4.1)	492
c-jet a	0.082(±0.019)	215.9(±13.2)	136
c-jet b ³	0.083(±0.016)?	128.6(±10.9)?	138?
c-jet d	0.138(±0.016)	237.9(±6.6)	229
x	0.049(±0.021)	343.6(±24.4)	81
y	0.189(±0.005)	59.5(±1.6)	314
z	0.111(±0.005)	66.6(±2.7)	184

¹Assuming a distance of 350 pc to HH 46/47.

²Apparent motion of complex using the cross correlation technique (see text).

³For a possible explanation of these rather anomalous results see text

REFERENCES

- Davis, C.J., Eisloffel, J., & Smith M.D. 1996, ApJ, 463, 246
- Davis, C.J., & Smith M.D. 1995, A&A, 443, L41
- Davis, C.J., & Smith M.D. 1996, A&A, 309, 929
- Dopita, M.A., Schwartz, R.D., & Evans, I. 1982, ApJ, 263, L73
- Downes, T.P., & Ray, T.P. 1998, in preparation

- Edwards, S., Ray, T. P., & Mundt, R. 1993, in *Protostars and Planets III*, eds. E. Levy & J. Lunine, (University of Arizona Press), 567
- Eisloffel, J. 1997, in *Herbig-Haro Outflows and the Birth of Low Mass Stars*, IAU Symposium No. 182, eds. B. Reipurth & C. Bertout, (Dordrecht: Kluwer Academic Publishers), 93
- Eisloffel, J., Davis, C. J., Ray, T. P., & Mundt, R. 1994, *ApJ*, 422, L91
- Eisloffel, J., Smith, M.D., Davis, C.J., & Ray, T.P. 1996, *AJ*, 112, 2087
- Eisloffel, J., & Mundt, R. 1994, *A&A*, 284, 530
- Everett, M.E. 1997, *ApJ*, 478, 246
- Franco, G.A.P. 1990, *A&A*, 227, 499
- Gredel, R. 1996, *A&A*, 305, 582
- Heathcote, S, Morse, J.A., Hartigan, P., Reipurth, B., Schwartz, R.D., Bally, J., & Stone, J.M. 1996, *AJ*, 112, 1141
- Mundt, R., & Fried, J.W. 1983, *ApJ*, 274, L83
- Noriega-Crespo, A., Garnavich, P.M., Curiel, S., Raga, A.C., & Ayala, S. 1997, *ApJ*, 486, L55
- Olberg, M., Reipurth, B., & Booth, R.S. 1992, *A&A*, 259, 252
- Padman, R., Bence, S., & Richer, J. 1997, in *Herbig-Haro Outflows and the Birth of Low Mass Stars*, IAU Symposium No. 182, eds. B. Reipurth & C. Bertout, (Dordrecht: Kluwer Academic Publishers), 123
- Reipurth, B., & Heathcote, S., 1991 *A&A*, 246, 511
- Schwartz, R., Jones, B.F., & Sirk, M. 1984, *AJ*, 89, 1735
- Smith, M.D., & Brand, P.W.J.L., 1990, *MNRAS*, 242, 495
- Smith, M.D. 1991, *MNRAS*, 252, 378
- Smith, M.D. 1994, *MNRAS*, 266, 238
- Suttner, G., Smith, M.D., Yorke, H.W., & Zinnecker, H. 1997, *A&A*, 318, 595
- Taylor, S.D., & Raga, A.C., 1995 *A&A*, 296, 823
- Zinnecker, H., McCaughrean, M., & Rayner, J. 1997, in *Low Mass Star Formation – from Infall to Outflow*, eds. F. Malbet & A. Castets, (Observatoire de Grenoble), 198

Figures:

Fig. 1.— $2.12\mu\text{m}$ wide-field contour plot of the HH 46/47 outflow derived from our image taken in April 1997 (see text). The various knots used for the proper motion study are identified (see Table 1). The contour levels are at 2, 4, 6, 8, ... $10^{-18}\text{W m}^{-2}\text{arcsec}^{-2}$. Proper motion vectors are shown. HH 46, which is in part a reflection nebula, is indicated.

Fig. 2.— $2.12\mu\text{m}$ contour plot of the HH 46/47 counterjet at two epochs (November 1995 and April 1997). As in Fig. 1 the knots referred to in the text are identified and proper motion vectors are shown. Note the disappearance of knot c-jet e in the 1997 image. The somewhat spurious result for knot c-jet b is explained in the text. The contour levels increase in steps of 1.2 from a base level of $2.4 \times 10^{-18}\text{W m}^{-2}\text{ arcsec}^{-2}$.

Fig. 1

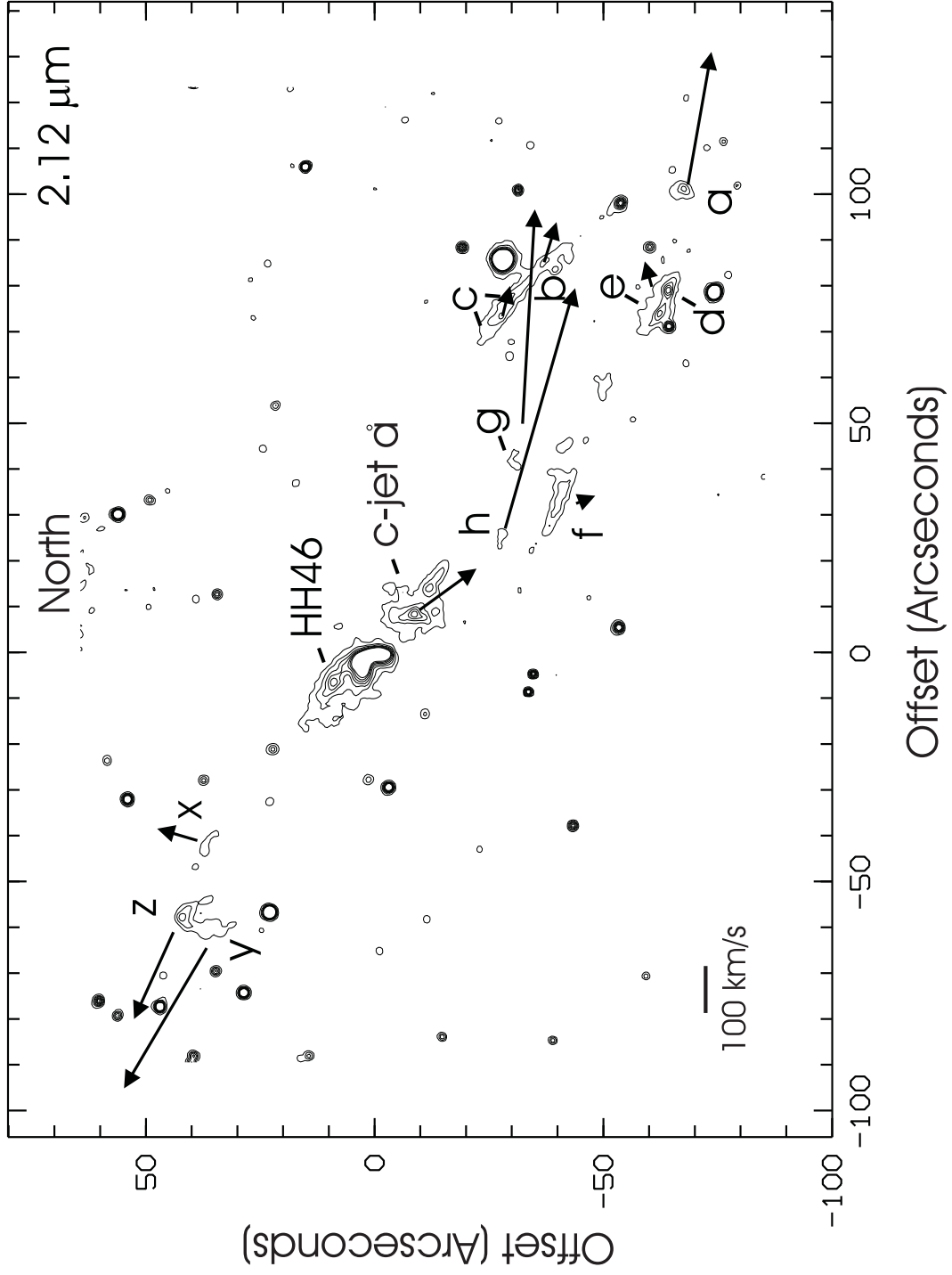


Fig. 2

